

The energy of muscle contraction. II. Transverse compression and work.*

David S. Ryan[†] Sebastián Domínguez^{‡§} Stephanie A. Ross[†]
 Nilima Nigam[‡] James M. Wakeling[†]

October 27, 2021

Abstract

In this study we reproduced this compression-induced reduction in muscle force through the use of a three-dimensional finite element model of contracting muscle. The model used the principle of minimum total energy and allowed for the redistribution of energy through different strain energy- densities; this allowed us to determine the importance of the strain energy-densities to the transverse forces developed by the muscle. Furthermore, we were able to study how external work done on the muscle by transverse compression affects the internal work and strain-energy distribution of the muscle. We ran a series of in silico experiments on muscle blocks varying in initial pennation angle, muscle length, and compressive load. As muscle contracts it maintains a near constant volume. As such, any changes in muscle length are balanced by deformations in the transverse directions such as muscle thickness or muscle width. Muscle develops transverse forces as it expands. In many situations external forces work to counteract these transverse forces. Muscle responds to external transverse compression while both passive and active. Transverse compression leads to a reduction in muscle thickness and pennation angle when the muscle is passive, and a reduction to the longitudinal force in its line-of-action when the muscle is active. Greater transverse compression leads to greater force reduction. The muscle blocks used in our simulations decreased in thickness and pennation angle when passively compressed, and pushed back on the compression when they were activated. We show how the longitudinal force from the muscle reduces with increased compressive load and that this reduction is dependent on the pennation angle and muscle length. The compression-induced reductions in the longitudinal muscle force were largely due to the volumetric strain-energy density, which is function of the bulk modulus of the muscle tissue and the dilation of the tissue.

Keywords: muscle, energy, finite element model, compression, transverse, tissue, deformation, 3D

*This work was partially supported by the Natural Sciences and Engineering Research Council of Canada and the Comisión Nacional de Investigación Científica y Tecnológica of Chile.

[†]Department of Biomedical Physiology and Kinesiology, Simon Fraser University, Burnaby, BC, Canada

[‡]Department of Mathematics, Simon Fraser University, Burnaby, BC, Canada

[§]Corresponding author: domingue@sfu.ca

1 Introduction

Muscles change in length and develop longitudinal force when they contract, and these result in internal work being done within the muscle. Muscles additionally expand and develop forces in transverse directions, again resulting from internal work. However, the transverse action of muscle is rarely studied. In this paper we show how longitudinal and transverse forces and deformations of the muscle are coupled via the internal energy of the muscle, and in particular through the redistribution of energy across different forms of strain-energy potentials.

Shape changes and muscle forces occur in all three dimensions when muscles contract. As a muscle shortens, it must increase in girth or cross-sectional area in order to maintain its volume (Zuurbier and Huijing, 1993; Böl et al., 2013; Randhawa and Wakeling, 2015). Transverse expansions of contracting muscle have been reported in both animal (Brainerd and Azizi, 2005; Azizi et al., 2008) and human studies (Maganaris et al. 1998; Randhawa et al., 2013; Dick and Wakeling, 2017), and transverse forces generated internally in the muscle can ‘lift’ weights during contraction (Siebert et al. 2014). Conversely, transverse loads that compress the muscle in its cross-section should be transferred to forces and changes in length along the line-of-action of the muscle.

The force that a muscle develops in its line-of-action depends on pressure and external loads applied in the transverse direction. Various researchers have used models of fibre-wound helical tubes (mimicking the endomysium and perimysium of the extracellular matrix) to explain the transfer of radial to longitudinal forces and deformations in the muscle (Azizi et al. 2017; Sleboda et al. 2017, 2019). Loading the extracellular matrix by increasing the volume of the semimembranosus muscle of the bullfrog, using osmotic pressure, increases the passive force in the line-of-action of the muscle (Sleboda et al. 2017; 2019). Limiting radial expansion of muscle by more circumferentially oriented fibres in the helix reduces the extent to which muscle can shorten, and placing a stiff tube around contracting frog plantaris muscle reduces both how much the muscle shortens and work done in the line-of-action (Azizi et al. 2017).

Transverse external loads act to compress passive muscle as they do mechanical work on the tissue. Compression of passive muscle has been described for isolated medial gastrocnemius in rats (Siebert et al. 2014, 2016) and for gluteus maximus (Linder-Ganz et al. 2007) and medial gastrocnemius (Stutzig et al. 2019; Ryan et al. 2019) muscles in humans. Muscles bulge to resist the transverse loads when they activate and work is generated from forces that develop in the transverse direction. The work generated from these transverse forces can be thought of as ‘lifting work’, especially if it is working against gravity (see the Methods for the formal definition). The muscle volume-specific energy involved in this ‘lifting work’ from the medial gastrocnemius has been approximately $1.1\text{-}1.2 \times 10^3 \text{ J m}^{-3}$ (Siebert et al. 2014) in the rat, and $1.1 \times 10^3 \text{ J m}^{-3}$ in humans (Stutzig et al. 2019): it should be noted that in these experiments the plungers that applied the transverse load covered only about 20% is about 2 orders of magnitude less than the work that could be done by the longitudinal muscle force (Weis-Fogh and Alexander, 1977). This force in the line-of-action during muscle contraction is reduced when the muscle does work to resist the transverse loads (Siebert et al. 2014; 2018; Stutzig et al. 2019; Ryan et al. 2019), and the extent of this force reduction depends on the transverse force rather than the external load applied to the muscle (Siebert et al. 2016). Siebert and colleagues (2012) explained transverse muscle forces and bulging from previous data using a hydraulically driven model that transfers load between the transverse to longitudinal directions. They used an ellipsoidal geometry with constraints that governed anisotropy in the

deformations: their model indicated that anisotropy in the connective tissue was important for the transfer of loads between the transverse and longitudinal directions.

Muscles are additionally packaged together in anatomical compartments, and they squeeze on each other as they bulge during contraction. This caused a decrease in the force from the combined quadriceps in the rabbit when compared to the sum of the individual muscle forces if they were stimulated separately (de Brito Fontana et al. 2018, 2020), although the reasons for this were not clear. Not all muscles increase in thickness during isometric contractions, and thus we should not expect that every muscle will squeeze into neighbouring muscles when they activate. Muscles with lower pennation angles (< 15 degrees) tend to bulge, whereas more pennate muscle may thin as they activate (Randhawa et al. 2013; Wakeling et al. 2020).

The changes in muscle force with external loads are length-dependent. For example, the force in bullfrog semimembranosus was decreased at short lengths and increased at long lengths, when compared to the resting length, when a pressure cuff was applied around the muscle to apply transverse force (Sleboda et al. 2019). Sleboda and colleagues (2019) explained these findings using a helically wound model in which the muscle acts to return to a length at which the angle of the helical fibres returns to their ideal pitch of 55 degrees (Wainwright et al. 1976), and this pitch was assumed to occur at the muscle's resting length. In contrast, greater reductions in muscle force have been detected in human plantarflexor muscles when they are compressed while at longer lengths (knee extended; Siebert et al. 2018) than at a shorter length (knee flexed: Ryan and Siebert observations).

When muscles activate, they increase in their pennation angle both for shortening and for isometric contractions. Internal deformations additionally occur within muscle when it is compressed: external transverse loads cause a reduction in the mean fibre pennation angle (Wakeling et al. 2013), and a reduction to the extent the pennation angle increases when the muscle contracts (Ryan et al. 2019). We previously showed that the redistribution of strain-energy potentials within contracting muscle changes with the pennation angle (Wakeling et al. 2020), and it is likely that work done on and by the muscle generated by forces in the transverse direction would also affect the strain-energy potentials within the muscle. Thus, we would expect that the external compression affects the strain-energy potentials within the muscle, that in turn could explain the changes in force in the line-of-action. The redistribution between the forms of energy also depends on the muscle length (Wakeling et al. 2020), and this may drive an interaction between the muscle length and the force reduction that occurs with external load, however, this has not yet been examined. It is also likely that the strain-energy potentials and the transfer of external loads on the muscles will depend on the direction of the external load relative to the fibre pennation (for example, is the muscle compressed from its top or from its side within the transverse plane).

These recent studies have shown that muscle force changes when external transverse loads are applied to the muscle, and that this effect is length dependent. Theories have discussed how transverse forces are transferred to longitudinal forces through the properties of the connective tissue in the muscle (Smith et al., 2011; Sleboda et al. 2019). However, these studies have not explained how the deformation of muscle tissues due to external compression loads is affected by the internal geometry or by the direction of the applied load relative to the muscle fibres. Our previous description of muscle (Wakeling et al. 2020), that quantifies how strain-energy potentials in the contractile elements are redistributed throughout the muscle volume and the contractile force is redirected across the muscle tissue, is well suited to understand these

mechanics of muscle compression. The purpose of this study was to identify whether the altered muscle forces that occur with compression can be explained in terms of the strain-energy potentials within the muscle, and in particular to account for the role of muscle length, pennation angle and the direction of the external load on the changes to muscle force.

2 Methods

In this paper we present simulations to compare the changes in the internal energy and internal pressure of muscle tissue during an external compression. We modelled the muscle as a three-dimensional and nearly incompressible fibre-reinforced composite biomaterial. The presence of 1D fibres through the base-material, representing contractile elements, results in an overall anisotropic response of the muscle tissue. The formulation of our model used in all simulations is based on the balance of strain-energy potentials as presented in Wakeling et al. 2020, and was solved using the finite element method (FEM). The main change is that here we study the influence of external loading on muscle force output.

The internal pressure is related to the muscle volume and the volumetric strain energy-density Ψ_{vol} in the muscle:

$$\Psi_{vol}(\mathbf{u}, p, J) := \frac{\kappa}{4}(J^2 - 2\log(J) - 1) + p(J - I_3(\mathbf{F})), \quad (1)$$

and can be calculated from the first variation in the volumetric strain energy-density with respect to J :

$$p - \frac{\kappa}{2}(J - 1/J) = 0,$$

where κ is the bulk modulus of the tissue, J the dilation, and $I_3(\mathbf{F})$ the third invariant of the deformation tensor \mathbf{F} (Wakeling et al. 2020). Note that we use strain-energy potentials to compare between blocks for the most of the discussion because the muscle blocks in this study all had the same initial volume. Muscle can show small changes in volume when it contracts (Neering et al., 1991; Smith et al., 2011; Bolsterlee et al., 2017), and so we have modelled the muscle as a nearly incompressible tissue (Wakeling et al. 2020).

2.1 Muscle geometries and simulations

We constructed a series of blocks of parallel-fibred and unipennate muscle with cuboid geometries (30x10x10 mm) and no aponeurosis. The origin of the coordinate system was centred within the blocks for their initial configuration V_0 . The muscle blocks had faces in the positive and negative x, y, and z sides. We defined the length of the blocks as the distance between the positive and negative x-faces in the x-direction, and the thickness as the distance between the positive and negative z-faces in the z-direction. The muscle fibres were parallel to each other and the xz plane in V_0 , but oriented at an initial pennation angle β_0 (0-40 degrees) away from the x-direction. We set the initial length of the fibres to their optimal length ($\lambda_{iso} = 1$), and the normalized muscle length \hat{l} to 1 for the undeformed blocks in their initial configuration V_0 . The material properties for the muscle tissue were the same as for our previous study (Wakeling et al. 2020), and we continued to use a scaling factor *base* of 1.5 for the base-material stiffness.

In silico compression tests were conducted in a series of stages as shown in Fig. 1. The different steps in our compression tests can be listed as follows:

- (A) We initially fixed the -x face in all directions, fixed the -z face in the z axis only, and we applied a traction to the +x face to either stretch or shorten the passive muscle. This traction was applied in the direction normal to the +x face in the initial configuration V_0 .
- (B) Next, we changed the constraints on the -x face to fix it only in the x-direction, fixed the -z face in all directions and we compressed the passive muscle by applying a transverse load (traction) of 0, 5, 15 or 30 kPa, consistent with previous experimental loads (Ryan et al., 2019; Stutzig et al., 2019). This traction was either on the +z face for ‘top’ loading, or the traction was from both y-faces for ‘side’ loading.
- (C) Finally, we fixed both x-faces in the x-direction, maintained the z-constraint on the -z face, and maintained the transverse traction to compress the muscle. During this stage we ramped the activation \hat{a} from 0 to 100% over a series of 10 time-steps.

2.2 Mechanical and lifting work

The work done by the muscle tissues during deformation is defined in terms of the force developed by the muscle, denoted by F , at a given point and the displacement \mathbf{u} at the same point. The total work is then defined as

$$W_{int} := \int_V F \cdot \mathbf{u} dV,$$

where V is the current configuration of the muscle tissue, and the dot between the vectors denote the dot product. The external work done by the prescribed compression loads on parts of the surface of the muscle geometries, which we denote by S , are computed as

$$W_{ext} := \int_S p_0 \hat{\mathbf{n}} \cdot \mathbf{u} dS,$$

where $p_0 \hat{\mathbf{n}}$ is the transverse force of the external compression and $\hat{\mathbf{n}}$ is the normal unit vector on the surface S . During activation of the muscle fibres the internal force may be greater than the force on the system from external loads on the surface S . In such cases, one can see that the muscle surface pushes back as the external compression load can no longer compress the tissues. The non-zero force that pushes back on the surface of the muscle, denoted by F_{lift} , defines a non-zero work which is done by the tissues. We refer to this work as the ‘lifting work’ of the muscle. The ‘lifting work’ is defined as

$$W_{lift} := \int F_{lift} \cdot \mathbf{u} dS.$$

2.3 Post-processing and data analysis

The FEM model calculates tissue properties across a set of 128,000 quadrature points within each muscle block. We defined an orientation for the fibres at each quadrature point. The pennation angle β_0 in the undeformed and current β states were calculated as the angle between the fibre orientations and the x-axis: this is an angle in 3D space, similar to the 3D pennation angles defined by Rana et al. 2013. We calculated forces F as the magnitude of

force perpendicular to a face on the muscle. The longitudinal muscle force in the line-of-action is denoted by F_x .

The strain-energies are initially calculated as strain energy-densities y , which are the strain-energy for a given volume of tissue, in units J m^{-3} . We compute the total strain-energy of the tissue. The strain-energy potential U is the strain-energy in the tissue, in units of Joules. We calculated U at each given state by integrating y across the volume of muscle tissue at that state. We computed volumetric, muscle base-material, muscle active-fibre, and muscle passive-fibre strain-energy potentials: U_{vol} , U_{base} , U_{act} , U_{pas} , respectively (see Appendix A in Wakeling et al. 2020).

3 Results

When the external load was applied to the passive muscle blocks on the z-face ('top' loading), the blocks decreased in their thickness in the z-direction, and also in their pennation angle. The extent of this compression increased with the external load. There was a minor effect of the pennation angle β_0 on this passive compression, with blocks at intermediate pennation angles of $\beta_0 = 20$ or 30 degrees compressing slightly more than the parallel fibred block, or the $\beta_0 = 40$ degrees block. The increases in tissue compression with increases in external transverse load are consistent with experimental measures using compression bandages (Wakeling et al. 2013) or weighted plungers on the medial gastrocnemius (Stutzig et al. 2019), and due to sitting on the gluteus maximus in humans (Linder-Ganz et al. 2007). Note that the internal pressure in the passive muscle block decreased with increasing external transverse load (Fig. 2b).

The internal pressure increased as the muscle activated. The internal pressure for the maximum activation state of $\hat{a} = 1$ was 37 ± 20 kPa (mean \pm S.D., $N = 60$) across all geometries and transverse loads, which is within the range of intramuscular pressures measured for muscle contractions: 13-40 kPa in the frog gastrocnemius, 27 kPa for the soleus (Aratow et al. 1993) and 30 kPa for the tibialis anterior in humans (Ates et al. 2018). However, the external transverse load was not directly proportional to the increase in the internal pressure in the muscle blocks (Fig. 2b and 3). Indeed, the coefficient of determination between external transverse load and the internal pressure was $r^2 = 0.052$ for all states ($N=600$), and $r^2 = 0.042$ for the fully active state ($N=60$) in these simulations.

The volumetric strain energy-density varies with both muscle length and pennation angles (Fig. 4) and cannot be predicted just from the activation state of the muscle (Wakeling et al. 2020). Across the range of pennation angles, activations, and muscle lengths used for the compression simulations in this study, the coefficient of variation for the volume of the muscle blocks was 0.02. By contrast, the range of the volumetric strain energy-densities of the muscle blocks was much larger with a coefficient of variation of 1.00. It is this greater range of volumetric strain energy-densities that drove the changes in internal pressure of the muscle (Fig. 3). Strain energy-density develops in the active fibres within the muscle (that represent the contractile elements) when the activation state increases, and is subsequently redistributed across the volumetric, base-material and passive-fibre strain energy-densities (Wakeling et al. 2020). We have also found that the volumetric strain energy-density varies with muscle length and pennation angle, and so too the internal pressure varies with length and pennation angle. This is a result of the nearly incompressibility nature of our model. As muscle tissues are allowed to change volume during contraction, the dilation J changes, causing the volumetric

strain energy-density to change (see Equation 1 in Methods section for the formal definition of this strain energy-density in terms of the dilation). Changes in both muscle length and pennation cause changes in the volume and therefore local changes in the dilation. With the definition of the internal pressure, we see that it also varies with muscle length and pennation angle. However, we noted that internal pressure does not possess a direct relation with the external transverse load: this is illustrated in Fig. 3 where each given transverse load can cause a range of different internal pressures depending on the length or pennation angle of the muscle block being compressed. Note that this highlights important considerations for interpreting experimental data (Wakeling et al. 2013; Siebert et al. 2016, de Brito Fontana et al. 2018; Sleboda et al. 2019) where muscle is compressed using transverse external loads, because the internal pressure in the muscle may not be directly related to the extent of the external load.

The compressed muscle blocks changed in thickness when they were activated (Fig. 5A). The least pennate muscle blocks ($\beta_0 \leq 10$ degrees) increased in thickness (bulged) when they were activated, and the more pennate blocks ($\beta_0 \geq 20$ degrees) decreased in thickness. This difference in the direction of bulging was consistent with previous experimental (Maganaris et al., 1998; Randhawa et al., 2013; Randhawa and Wakeling, 2013, 2018; Raiteri et al. 2016) and modeling results (Wakeling et al. 2020). The parallel fibred block of muscle ($\beta_0 = 10$ degrees) bulged during activation, however there was minimal effect of the transverse load on this bulging. By contrast, contracting against greater transverse loads increased the bulging and the pennation angle of the pennate muscle blocks (Fig. 5B). However, the pennation angle never returned to its undeformed values of β_0 during these compressions and contractions. All the pennate blocks ‘lifted’ the external load when it was applied from the ‘top’, or in other words, the distance between the z-faces increased when the load was applied to the z-face. The ‘lifting work’ against this external load was the lowest for the $\beta_0 = 10$ degrees at $0.3 \times 10^3 \text{ J m}^{-3}$, and increased to $1.4 \times 10^3 \text{ J m}^{-3}$ for $\beta_0 = 40$ degrees when measured in comparison to the unloaded state. This range of ‘lifting work’ spans the values recorded in experimental studies: $1.1\text{-}1.2 \times 10^3 \text{ J m}^{-3}$ (Siebert et al. 2014) in rats, and $1.1 \times 10^3 \text{ J m}^{-3}$ in humans (Stutzig et al. 2019), where this work is expressed as a muscle volume-specific energy density.

The strain-energy increased in the muscle during contraction (Fig.4). The strain-energy redistributed across different strain-energy potentials (volumetric, base-material, active-fibre and passive-fibre) in a complex manner that depended on the muscle length, activation and pennation angle, similar to our previous study (Wakeling et al. 2020). Muscles with greater initial pennation angle β_0 developed much larger base-material strain-energy potentials (Fig. 4), due to the greater shortening of the muscle fibres, in a manner also seen in our previous study (Wakeling et al. 2020). The volumetric strain-energy potential was larger at longer muscle lengths \hat{l} for $\beta_0 \leq 20$ degrees as also shown in our previous study (Wakeling et al. 2020), but the relation was more complex at $\beta_0 \geq 30$ degrees (Fig. 4). The volumetric strain-energy potential was reduced with greater transverse external loads for most muscle lengths and pennation angles β_0 , apart from at $\beta_0 = 40$ degrees and $\hat{l} = 1.0$, and at β_0 of 30-40 degrees and $\hat{l} = 0.9$ (Fig. 4).

The force F_x developed in the line-of-action of the muscle varied with muscle length, pennation angle and external load (Fig. 6). For comparative purposes, the change in force ΔF_x is expressed relative to the maximum uncompressed force for that muscle at length \hat{l} and pennation angle β_0 , and ΔF_x was normalized to the maximum uncompressed force that occurred at the resting length $\hat{l} = 1.0$ for that pennation angle β_0 . We also compared here the results for

transverse loading from the ‘top’ (z-) and the ‘side’ (y-) direction. The force ΔF_x was reduced with compression for muscle blocks with $\beta_0 \leq 20$ degrees, with the force reduction becoming greater for increased transverse loads. The reduction in force was greater when the load was from the top than from the side. Patterns of force reduction ΔF_x differed for the more pennate blocks: for the $\beta_0 = 40$ degrees block the force actually increased with transverse loading from the top. For the transverse loading from the top, the muscle blocks showed the greatest force reduction at their initial length $\hat{l} = 1.0$ for $\beta_0 = 0$ degrees. The greatest force reduction at the short muscle length $\hat{l} = 0.9$ occurred at $\beta_0 = 10$ degrees, and the greatest force reduction at the longest length $\hat{l} = 1.1$ occurred for $\beta_0 = 30$ degrees, with these patterns varying slightly when the load was applied to the sides of the blocks. Here we show that the force reduction for muscle depends in a complex manner on the length, pennation angle and direction of the transverse load, with this effect being due to the way in which the strain-energy potentials are redistributed across the muscle during these externally loaded contractions (Fig. 4).

The contributions of the different strain-energy potentials to the force F_x in the line-of-action of the muscle are shown in Fig. 7. For muscle with low to moderate initial pennation $\beta_0 \leq 20$ degrees, the largest reduction in force that occurred with external transverse load was from a reduced contribution from the volumetric strain-energy potential. Reductions in the volumetric strain-energy potential were less pronounced with external transverse load for the highest pennation angle of $\beta_0 = 40$ degrees, however at this pennation angle the muscle force actually increased at the highest transverse load and shortest length: this can be attributed to the substantial increase of the contribution from the base- material strain-energy potential that occurred for this state.

4 Discussion

In this study we used the finite element method (FEM) to evaluate a 3D model of skeletal muscle, based on the principles of continuum mechanics, to probe the relation between external transverse load on the muscle and the force that it can develop in its line-of-action as well as the internal work done by the tissues. The FEM model contained a series of constitutive relations that are based on phenomenological descriptions of contractile elements and tissue properties (see details of the model in Wakeling et al. 2020): none of these relations were specifically derived from or optimized to the transverse response of muscle contractions, in contrast to previous models (Randhawa and Wakeling, 2015; Siebert et al. 2012, 2014, 2018). Nonetheless, the model predicted many of the general features of the compression response that have been previously reported, and so these general features emerge from the physical principles that govern 3D deformations in muscle tissue. We chose the main compression direction to be from the ‘top’ which is an external load acting parallel to the plane of the muscle fibres and is the direction that was tested in previous uniaxial loading in both animal (Siebert et al. 2014, 2016) and human experiments (Ryan et al. 2019; Stutzig et al. 2019). With this compression from the top, our model predicted that passive muscle tissue would decrease in thickness (Fig. 2), and the fibres would decrease in pennation angle, supporting experimental results (Ryan et al. 2019). When the compressed muscle was activated, the model predicted that it would increase in thickness to ‘lift’ the external load, generating lifting work (Siebert et al. 2014) in the same range $0.3\text{-}1.4 \times 10^3 \text{ J m}^{-3}$ as experimental measures $1.1\text{-}1.2 \times 10^3 \text{ J m}^{-3}$ (Siebert et al. 2014; Stutzig et al. 2019), where this work is expressed as a muscle volume-specific energy density.

The model in this study highlights the length-dependency of reductions in muscle force with applied transverse loads. Most of our simulations showed a force reduction with transverse load, and the extent of the force reduction was length-dependent at any given pennation angle. However, some of the conditions at the highest pennation angles $\beta_0 = 30 - 40$ degrees showed increases in force (Fig. 6). The length dependency derives from both the fibre and the base properties of the muscle model. The fibres are encoded as contractile elements that have length-dependent force properties for both the active-fibre and passive-fibre components, and the base properties are governed by both the volumetric and base-material relations (Rahemi et al. 2014; Wakeling et al. 2020). The combination of the volumetric and base-material properties results in a tissue that tends to return to its initial state (volume and shape) after it has been deformed, and this is a similar property to the helical-wound representation of connective tissue modelled by Sleboda and colleagues (2019). It should be noted that the initial undeformed state that these models return to is a discretionary choice between studies, and so it should not be expected that the exact same length-dependency of the compression-force reduction would occur across the different models. Indeed, this is the case where the helical model predicts force increase at longer lengths (Sleboda et al. 2019), whereas our model predicts these increases at the largest pennation angles (Fig. 6).

The pennation angle of the muscle had a pronounced effect on the muscle response to compression in terms of tissue deformation (Fig. 5), strain-energy potentials (Fig. 4), and the changes in muscle force (Fig. 6). When pennate muscle contracts, the fibres rotate to greater pennation angles as they shorten (Fukunaga et al. 1997; Maganaris et al. 1998). Muscle fibres act to draw the aponeuroses together (or for these simulations, the z-faces) as they shorten, which tends to decrease the muscle thickness. However, the fibres increase in girth during shortening in order to maintain their volume (Rahemi et al., 2014, 2015). The increase in girth may be in either the width or thickness direction, and indeed the relative deformations may vary between muscles (Randhawa and Wakeling, 2015, 2018) due to stress asymmetries through the muscle (Wakeling et al. 2020). However, a general effect is for the muscle to increase in pennation angle to allow their fibres to fit within the enclosed volume of the muscle tissue (Zuurbier and Huijing, 1993; Fukunaga et al., 1997). This increase in pennation angle tends to increase the muscle thickness (Randhawa and Wakeling, 2018), which in turn resists muscle compression acting from the ‘top’ direction and contributes to the lifting work of the muscle. The results from these simulations support this explanation. We additionally show how the strain-energy potentials redistribute within the muscle in a pennation- dependent manner (Fig. 4; Wakeling et al. 2020). Thus, the response to the compression and the internal work that can be done by the muscle will also be pennation dependent, due to the altered balance of strain-energy potentials within the muscle. We show here that the force reduction that occurs with transverse loading of the muscle seems particularly dependent on the volumetric strain-energy potential (Fig. 7), that in turn varies with pennation angle and the direction of the external load relative to the fibres (side or top: Fig. 4).

Strain-energy potentials develop during contraction and are distributed through the muscle (Wakeling et al. 2020). When the muscle contracts it increases in its free energy, with this energy being derived from the hydrolysis of ATP to ADP within the muscle fibres (Woledge et al., 1985; Aidley, 1998). The active-fibre strain-energy potentials are redistributed to passive-fibre strain- energy potentials and then to the base material strain-energy potential that develops in the bulk muscle tissue within the muscle fibres (excluding the myofilament fraction), con-

nective tissue surrounding the muscle fibres such as the extracellular matrix, and in sheets of connective tissue that form the aponeuroses and internal and external tendons. Energy is also used to change the muscle volume. Whilst muscle is often assumed to be incompressible, small changes in volume can occur in fibres (Neering et al., 1991), bundles of fibres called fascicles (Smith et al., 2011), and in whole muscle (Bolsterlee et al., 2017): these changes in volume are energy-consuming processes. The volumetric strain-energy potential, which accounts for an energetic penalty to any changes in volume that occur, builds up as the muscle is activated and shows slight increases in volume (Wakeling et al. 2020). The transverse external loads in this study act to compress the volume of the muscle (Fig. 2A). These changes in volume relate to changes to the volumetric strain-energy potential as the muscle is compressed. The volumetric strain-energy potential contributes to the contractile force F_x in the line-of-action for all bar the $\beta_0 = 40$ degrees condition at its shortest length. Thus, the compression-induced reductions in volumetric strain-energy potential result in the reductions to force in the line-of-action during the muscle contractions (Fig. 7).

The volumetric strain-energy potential is arguably the least-well characterized component of the internal energy in the muscle in our simulations. The extent of the increase in volume and the volumetric strain-energy potential is related to the choice of the bulk modulus κ of the tissue. A constitutive equation to calculate the volumetric strain-energy potential has not been defined for muscle tissue, and so we used a general form (equation 1) that is used for compressible neo-Hookean material (see, e.g. Pelteret 2012). Here we used a value of $\kappa = 10^6$ Pa that was consistent with previous studies (Rahemi et al., 2014, 2015, Wakeling et al. 2020). We previously showed that this κ resulted in volume changes of 2%-4% during contraction of fully active parallel muscle fibres. Nonetheless, a previous study showed that κ can be varied across a wide range of magnitudes and still result in similar predictions of tissue deformation (Gardiner and Weiss, 2001). Given the apparent importance of the volumetric strain-energy potential to the modulation of contractile force in response to muscle compression, establishing muscle-specific constitutive equations for the volumetric strain energy-density and values for the bulk modulus will be an important area of future investigation.

Conflict of Interest The authors declare that the research was conducted in the absence of any commercial or financial relationships that could be construed as a potential conflict of interest.

Author Contributions DR, NN, JW contributed to the study design. DR, SD, SR, NN, JW contributed to the model development. DR ran all the simulations for the paper and data analysis. DR and JW contributed to the first draft of the manuscript. DR, SD, SR, NN, JW contributed to final manuscript preparation.

Funding We thank the Natural Sciences and Engineering Research Council of Canada for Discovery Grants to J.M.W. and N.N., and an Alexander Graham Bell Canada Graduate Scholarship-Doctoral to S.A.R. We are also grateful for funding to S.D. from Comisión Nacional de Investigación Científica y Tecnológica of Chile through Becas-Chile.

Acknowledgments We thank Tobias Siebert for extensive discussions and inspiration about the mechanics of muscle compression.

References

- Aidley, D. J. (1998). *The Physiology of Excitable Cells*, 4th Edition. Cambridge: Cambridge University Press.
- Aratow, M., Ballard, R., Crenshaw, A., Styf, J., Watenpaugh, D., Kahan, N., and Hargens, A. (1993). Intramuscular pressure and electromyography as indexes of force during isokinetic exercise. *J. Appl. Physiol.*, 74, 2634-2640.
- Azizi, E., Brainerd, E., and Roberts, T. (2008). Variable gearing in pennate muscles. *PNAS*, 105(5), 1745-1750.
- Azizi, E., Deslauriers, A. R., Holt, N. C., and Eaton, C. E. (2017). Resistance to radial expansion limits muscle strain and work. *Biomech. Model. Mechanobiol.* 16, 1633-1643. doi: 10.1007/s10237-017-0909-3
- Böl, M., Leichsenring, K., Weichert, C., Sturmat, M., Schenk, P., Blickhan, R. and Siebert, T. (2013). Three-dimensional surface geometries of the rabbit soleus muscle during contraction: input for biomechanical modelling and its validation. *Biomech. Model. Mechanobiol.* 12, 1205-1220. doi: 10.1007/s10237-013-0476-1
- Bolsterlee, B., D'Souza, A., Gandevia, S. C., and Herbert, R. D. (2017). How does passive lengthening change the architecture of the human medial gastrocnemius muscle? *J. Appl. Physiol.* 122, 727-738. doi: 10.1152/jappphysiol.00976.2016
- Brainerd, E. L., and Azizi, E. (2005). Muscle fiber angle, segment bulging and architectural gear ratio in segmented musculature. *J. Exp. Biol.* 208, 3249–3261. doi: 10.1242/jeb.01770
- de Brito Fontana, H., de Campos, D., Sawatsky, A., Han, S.-W., and Herzog, W. (2020). Why do muscles lose torque potential when activated within their agonistic group? *J. Exp. Biol.*, 223(1), jeb213843. doi:10.1242/jeb.213843
- de Brito Fontana, H., Han, S. W., Sawatsky, A., and Herzog, W. (2018). The mechanics of agonistic muscles. *J. Biomech.* 79, 15-20. doi: 10.1016/j.jbiomech.2018.07.007
- Dick, T. J. M., and Wakeling, J. M. (2017). Shifting gears: dynamic muscle shape changes and force- velocity behavior in the medial gastrocnemius. *J. Appl. Physiol.* 123, 1433–1442. doi: 10.1152/jappphysiol.01050.2016
- Fukunaga, T., Ichinose, Y., Ito, M., Kawakami, Y., and Fukashiro, S. (1997). Determination of fascicle length and pennation in a contracting human muscle in vivo. *J. Appl. Physiol.*, 82(1), 354–358. doi:10.1152/jappl.1997.82.1.354
- Gardiner, J. C., and Weiss, J. A. (2001). Simple Shear Testing of Parallel-Fibered Planar Soft Tissues. *J. Biomech. Eng.* 123, 170–175. doi: 10.1115/1.1351891
- Linder-Ganz, E., Shabshin, N., Itzchak, Y., Gefen, A., (2007). Assessment of mechanical conditions in sub-dermal tissues during sitting: a combined experimental-MRI and finite element approach. *J. Biomech.* 40, 1443–1454.
- Maganaris, C., Baltzopoulos, V., and Sargeant, A. (1998). In vivo measurements of the triceps surae complex architecture in man: implications for muscle function. *J. Physiol.* 512, 603-614. doi: 10.1111/j.1469-7793.1998.603be.x
- Neering, I. R., Quesenberry, L.A., Morris, V.A., and Taylor, S.R. (1991). Nonuniform volume changes during muscle contraction. *Biophys. J.* 59, 926–933. doi: 10.1016/S0006-3495(91)82306-2
- Pelteret, J. P., and McBride, A. (2012). The deal.II tutorial step-44: Three-field formulation for non- linear solid mechanics. doi: 10.5281/zenodo.439772

- Rahemi, H., Nigam, N., and Wakeling, J. M. (2014). Regionalizing muscle activity causes changes to the magnitude and direction of the force from whole muscles – a modeling study. *Front. Physiol.* 5:298. doi: 10.3389/fphys.2014.00298
- Rahemi, H., Nigam, N., and Wakeling, J. M. (2015). The effect of intramuscular fat on skeletal muscle mechanics: implications for the elderly and obese. *J. R. Soc. Interface* 12:20150364. doi: 1098/rsif.2015.0365
- Raiteri B.J., Cresswell A.G., and Lichtwark G.A. (2016) Three-dimensional geometrical changes of the human tibialis anterior muscle and its central aponeurosis measured with three-dimensional ultrasound during isometric contractions. *PeerJ* 4:e2260.
- Raiteri, B. J., Cresswell, A. G. and Lichtwark, G. A. (2016). Three-dimensional geometrical changes of the human tibialis anterior muscle and its central aponeurosis measured with three-dimensional ultrasound during isometric contractions. *PeerJ.* 4:e2260. doi: 10.7717/peerj.2260
- Rana, M., Hamarneh, G., and Wakeling, J. (2013). 3D fascicle orientations in triceps surae. *J. Appl. Physiol.* 115: 116–125, 2013
- Randhawa, A., and Wakeling, J. M. (2015). Multidimensional models for predicting muscle structure and fascicle pennation. *J. Theor. Biol.* 382, 57–63. doi: 10.1016/j.jtbi.2015.06.001
- Randhawa, A., and Wakeling, J. M. (2018). Transverse anisotropy in the deformation of the muscle during dynamic contractions. *J. Exp. Biol.* 221:jeb175794. doi: 10.1242/jeb.175794
- Randhawa, A., Jackman, M. E., and Wakeling, J. M. (2013). Muscle gearing during isotonic and isokinetic movements in the ankle plantarflexors. *Eur. J. Appl. Physiol.* 113, 437–447. doi: 10.1007/s00421-012-2448-z
- Ryan, D. S., Stutzig, N., Siebert, T., & Wakeling, J. M. (2019). Passive and dynamic muscle architecture during transverse loading for gastrocnemius medialis in man. *J. Biomech.* 86, 160–166. doi:10.1016/j.jbiomech.2019.01.054
- Siebert, T., Till, O., & Blickhan, R. (2014). Work partitioning of transversally loaded muscle: Experimentation and simulation. *Comp. Meth. Biomech. Biomed. Eng.* DOI: 10.1080/10255842.2012.675056
- Siebert, T., Günther, M., & Blickhan, R. (2012). A 3D-geometric model for the deformation of a transversally loaded muscle. *J. Theor. Biol.* 298(C), 116–121. doi:10.1016/j.jtbi.2012.01.009
- Siebert, T., Stutzig, N., and Rode, C. (2018). A hill-type muscle model expansion accounting for effects of varying transverse muscle load. *J. Biomech.* 66, 57–62. doi:10.1016/j.jbiomech.2017.10.043
- Sleboda, D. A., and Roberts, T. J. (2019). Internal fluid pressure influences muscle contractile force. *PNAS*, 5(3), 201914433–1778. doi:10.1073/pnas.1914433117
- Sleboda, D. A., and Roberts, T. J. (2017). Incompressible fluid plays a mechanical role in the development of passive muscle tension. *Biol. Lett.* 13, 20160630. doi: 10.1098/rsbl.2016.0630
- Smith, L. R., Gerace-Fowler, L., and Lieber, R. L. (2011). Muscle extracellular matrix applies a transverse stress on fibers with axial strain. *J. Biomech.* 44, 1618–1620. doi: 10.1016/j.jbiomech.2011.03.009
- Stutzig, N., Ryan, D., Wakeling, J. M., and Siebert, T. (2019). Impact of transversal calf muscle loading on plantarflexion. *J. Biomech.* 85, 37–42. doi:10.1016/j.jbiomech.2019.01.011
- Wainwright S. A., Biggs W. D., Currey J. D., and Gosline J. M. (1976). Mechanical design in organisms. John Wiley & Sons Inc
- Wakeling J. M., Ross S. A., Ryan D. S., Bolsterlee B., Konno R., Domínguez S., and Nigam N. (2020). The energy of muscle contraction. I. Tissue force and deformation during isometric

contractions. Submitted to *Frontiers Physiology* (special project on muscle ECM).

Wakeling, J. M., Jackman, M., and Namburete, A. I. (2013). The effect of external compression on the mechanics of muscle contraction. *J. Appl. Biomech.* 29, 360–364. doi:10.1123/jab.29.3.360

Weis-Fogh, T., and Alexander, R. M. (1977). “The sustained power output from straited muscle,” in *Scale Effects in Animal Locomotion*. ed T. J. Pedley (New York: Academic Press), 511-525.

Woledge, R. C., Curtin, N. and Homsher, E. (1985). *Energetic Aspects of Muscle Contraction*. *Monogr. Physiol. Soc.* 41, 1-357.

Zuurbier, C. J., and Huijing, P. A. (1993). Changes in muscle geometry of actively shortening unipennate rat gastrocnemius muscle. *J. Morphol.* 218, 167–180. doi:10.1002/jmor.1052180206

Figures

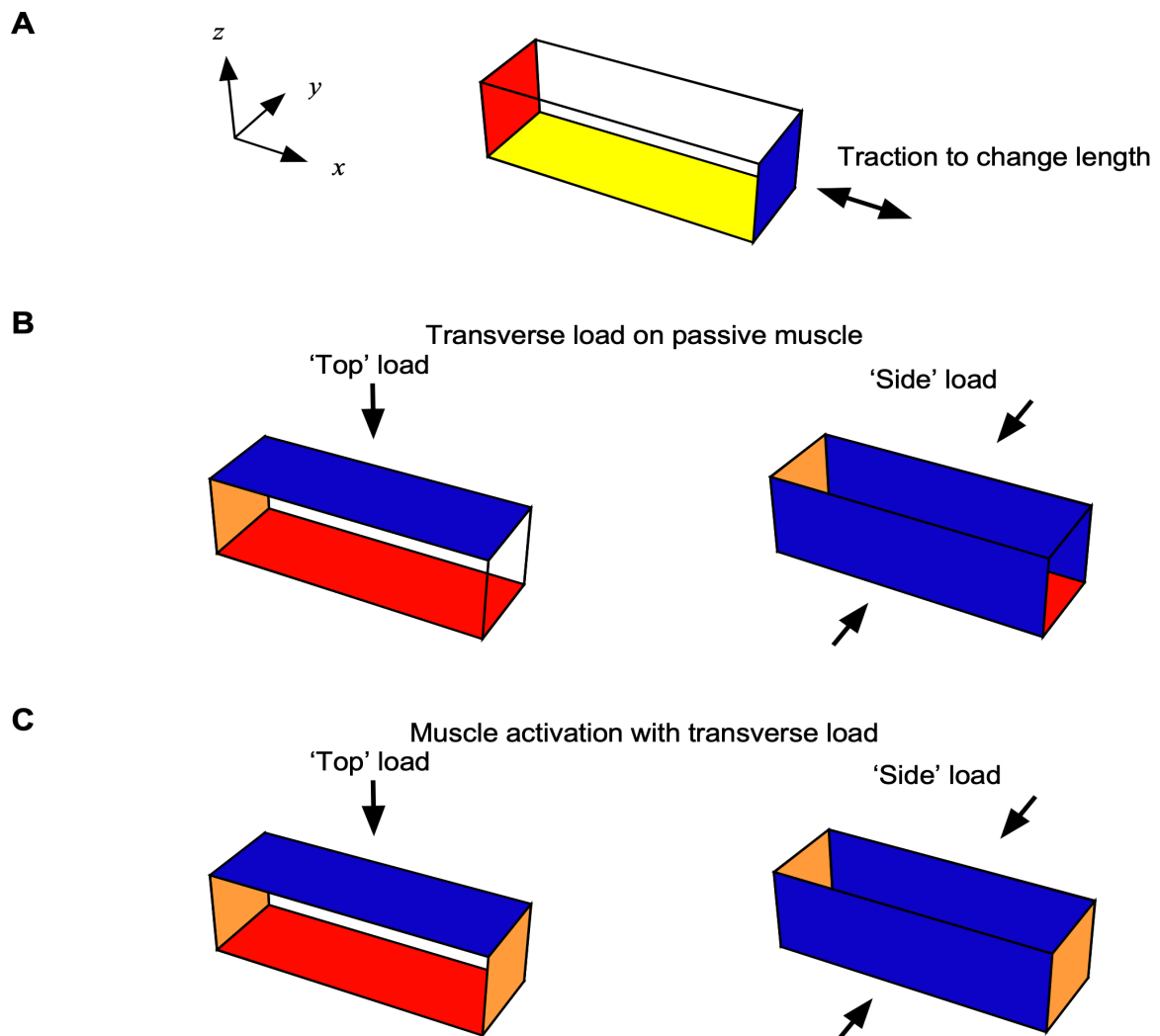


Figure 1: Boundary conditions for the three stages of the model. (A) Initially the $-x$ face of the muscle block was fixed in all directions (red), the $-z$ face was fixed in the z axis (yellow), and the $+x$ face had traction applied (blue) to shorten or lengthen the muscle. (B) For compression of the muscle the $-x$ face was fixed in the x axis (orange), the $-z$ face was fixed in all directions (red), and a transverse load (traction) was applied to the 'top' $+z$ -face (blue), or the 'side' y -faces (blue). (C) During activation the x faces were fixed in the x axis (orange), the $-z$ face was fixed in all directions (red), and the transverse load (traction) was maintained for the 'top' $+z$ -face (blue), or the 'side' y -faces (blue).

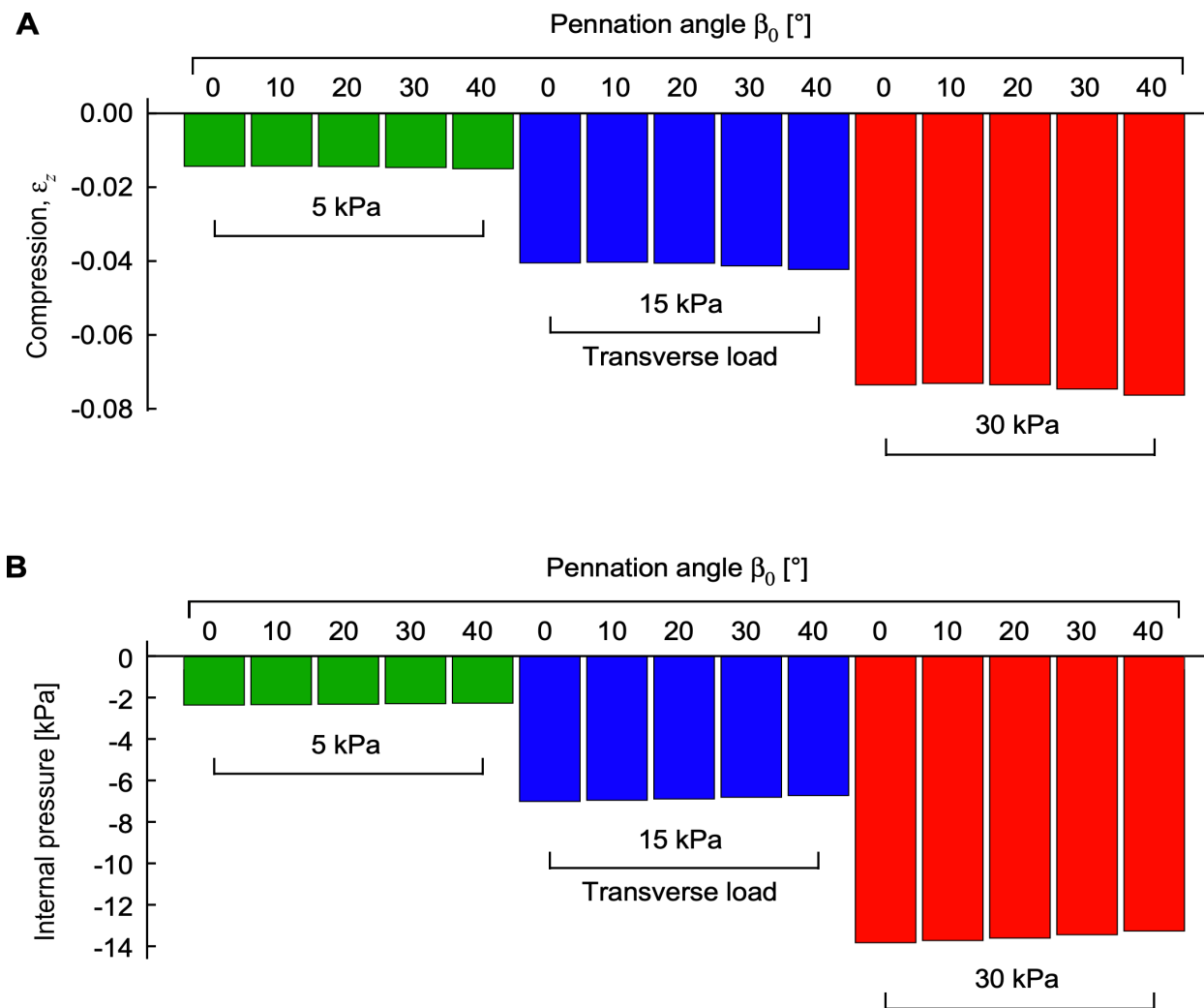


Figure 2. Compression and internal pressure in passive muscle blocks when transversely loaded.

Transverse loads were applied in the $-z$ direction to the $+z$ -face. Compression is shown as a strain between the z -faces relative to their uncompressed state (A). Internal pressure is shown relative to the uncompressed state (B). Transverse loads are distinguished by colour (green: 5 kPa, blue: 15 kPa, red: 30 kPa). For each transverse load, different blocks were compressed with initial pennation angles β_0 from 0 to 40°. Results are shown for blocks that were compressed at a muscle length of $\hat{l} = 1.0$.

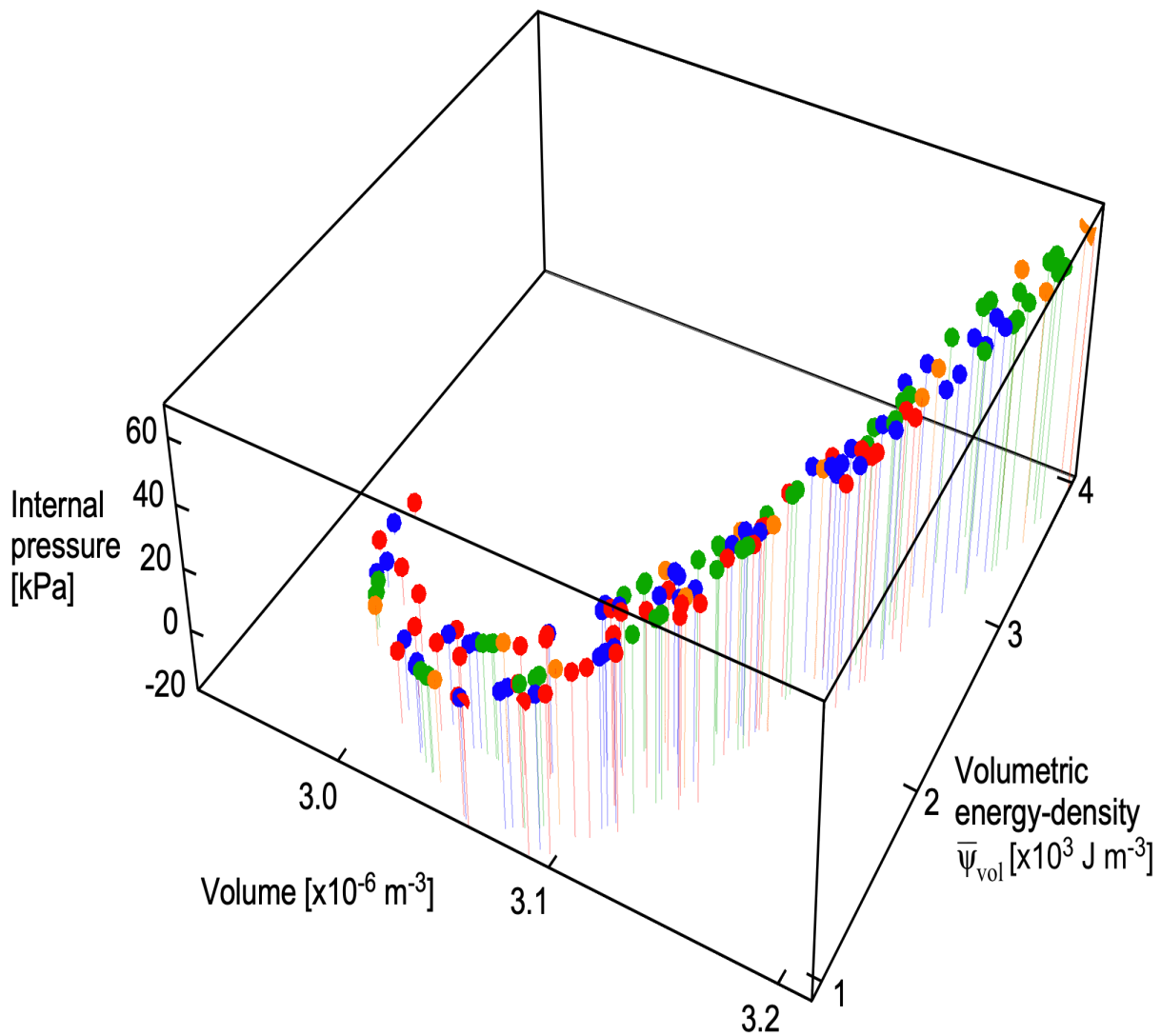


Figure 3. Internal pressure as a function of volume and strain energy-density. Points are shown for the maximum activation state for all muscle lengths and pennation angles. Transverse loads are distinguished by colour (orange: unloaded, green: 5 kPa, blue: 15 kPa, red: 30 kPa).

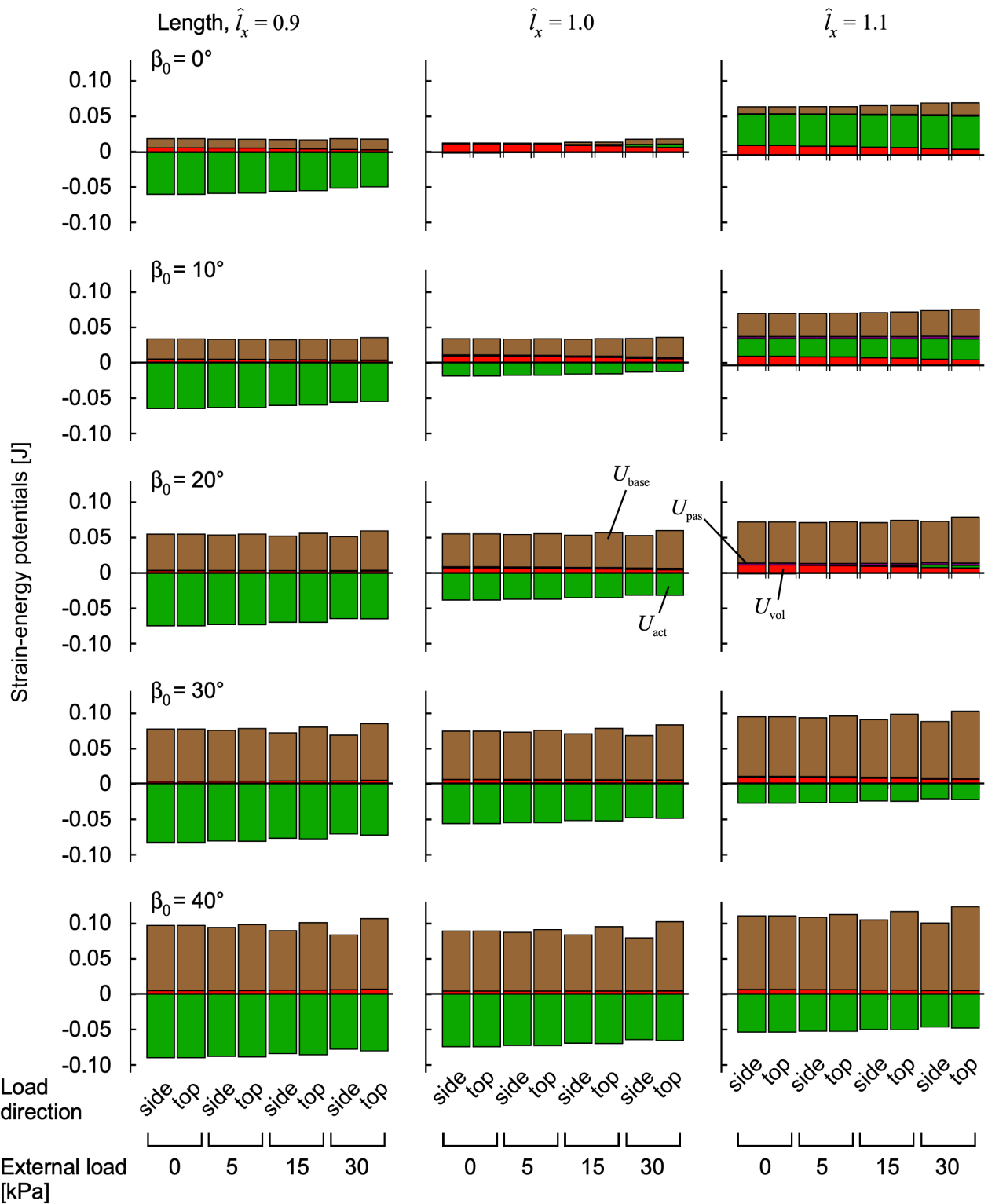


Figure 4. Strain-energy potentials during muscle contraction with transverse external load. Force in the line-of-action of the muscle blocks, measured on the x face. The muscle blocks were initially stretched or shortened to a new length using traction on the +x face, then loaded in a transverse direction and activated to 100%. Strain-energy potentials are: base-material, brown; volumetric, red; active-fibre, green and passive-fibre, purple.

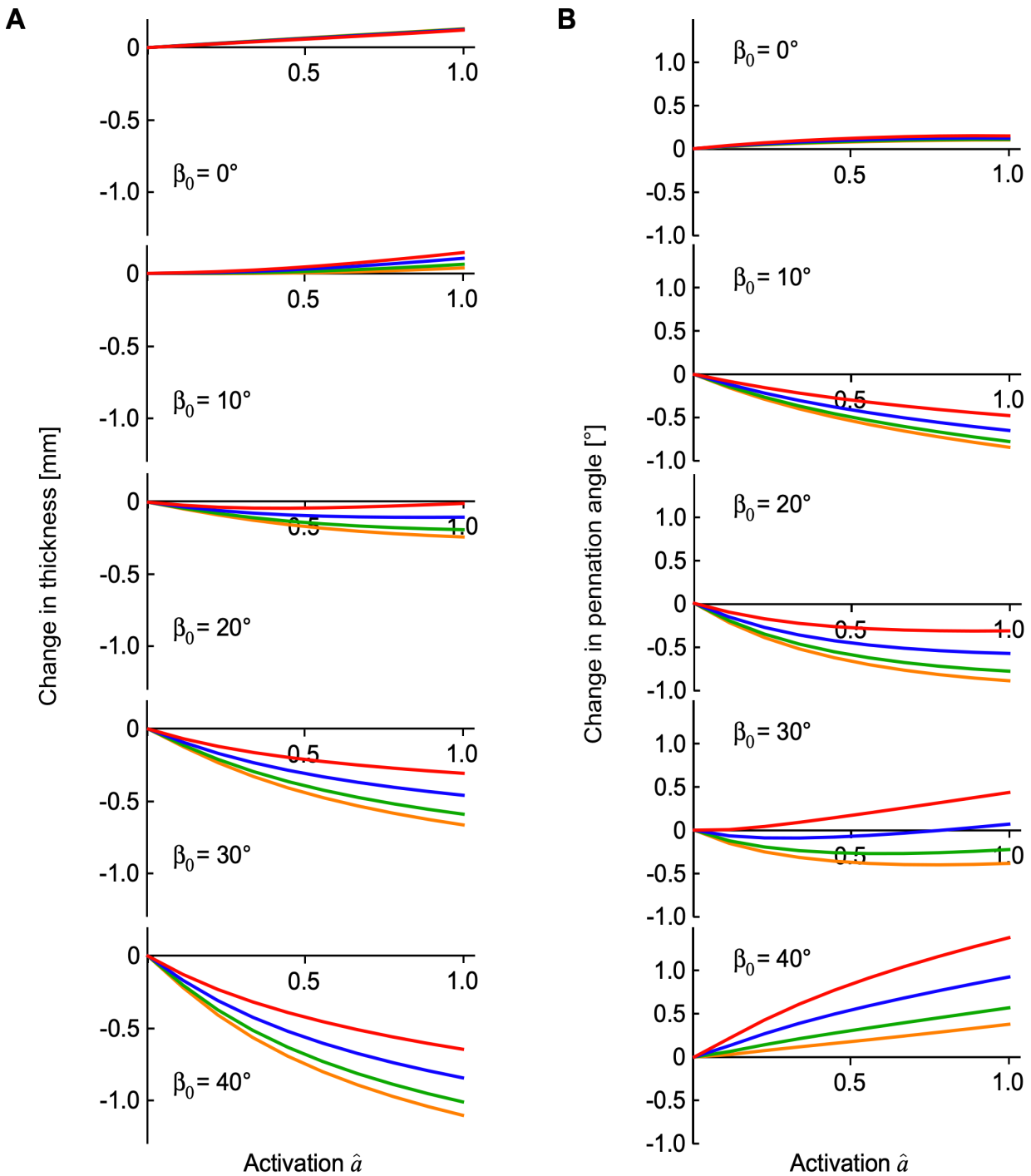


Figure 5. Changes in muscle thickness and pennation angle during contractions with external loads.

The transverse external loads were applied from the ‘top’ z -direction and are distinguished by colour (orange, 0 kPa; green: 5 kPa, blue: 15 kPa, red: 30 kPa). The change in thickness (A) is the change in distance between the $-z$ and $+z$ faces of the muscle blocks, and the change in pennation (B) is the difference in mean pennation angle of the muscle fibres, with both these parameters being calculated relative to the passive but compressed state. The results are shown for the muscle blocks at an initial length of $\hat{l} = 1.0$.

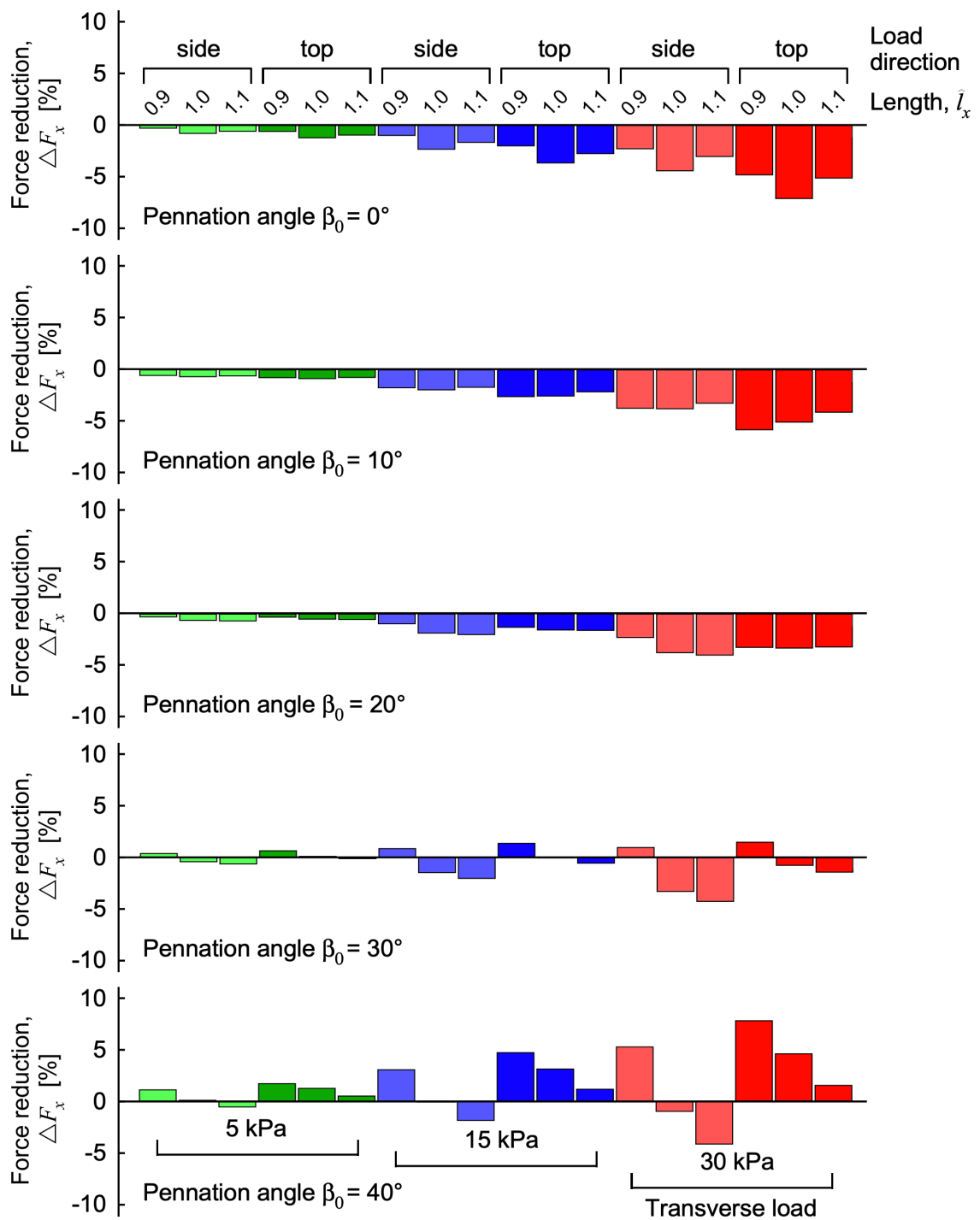


Figure 6. Reduction in longitudinal force during muscle contraction with transverse load. For each pennation angle the force reduction is shown relative to the unloaded state at each length, normalized to the maximum isometric force at a length of $\hat{l} = 1$ and activation of $\hat{a} = 1$. Transverse loads are distinguished by colour (green: 5 kPa, blue: 15 kPa, red: 30 kPa). Muscle blocks were tested at three lengths, \hat{l} , with compression in the y - (side) or z - (top) directions. For each transverse load, different blocks were compressed with initial pennation angles β_0 from 0 to 40° .

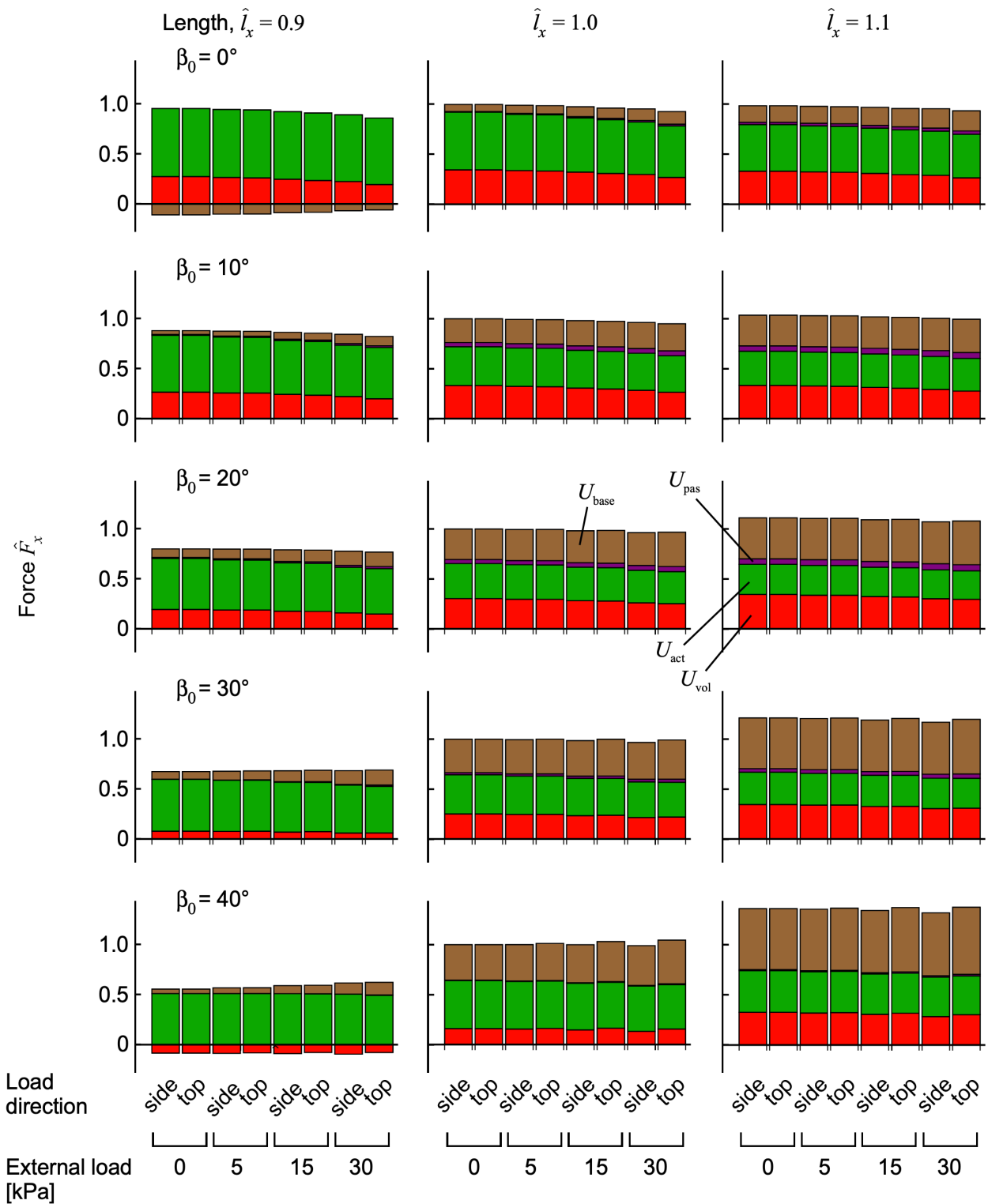


Figure 7. Components of force from the strain-energy potentials during muscle contraction with transverse external load. Force in the line- of-action of the muscle blocks, measured on the x face. The muscle blocks were initially stretched or shortened to a new length using traction on the +x face, then loaded in a transverse direction and activated to 100%. The force \hat{F}_x is normalized to the maximum force achieved for the unloaded muscle at normalized length $\hat{l}=1.0$, for each initial pennation β_0 .